

# 볼 엔드밀 제작을 위한 모델링 및 시뮬레이션

## Modeling and simulation for manufacturing of ball end mill

\*팜트롱탄<sup>1</sup>, 고성림<sup>2</sup>

\* Trung Thanh Pham<sup>1</sup>, #S. L. Ko<sup>2</sup> (slko@konkuk.ac.kr)

<sup>1,2</sup> 건국대학교 기계설계학과,

Key words: Ball end mill, helical flute, CNC grinding.

### 1. Introduction

Ball end mills are widely used in industry for high speed milling operation and machining three dimensional complicated surfaces, such as molds, sculptured dies, turbine blades and aerospace parts... Many kinds of ball end mill with various shapes and dimensions have been developed. Much work has been carried out on mathematical models for helical groove machining and the cutting edge curve of the cutting tool [1-4]. This paper presents about modeling and simulation for manufacturing of ball end mill using 5-axis CNC machine. Fig.1 shows the configuration of 5-axis CNC machine for manufacturing of ball end mill, which has 5 degrees of freedom: three axes in translation (X, Y, Z) and two axes in rotation (A, W). The computer program is developed to define the tool shapes of ball end mills, wheel geometry and generate the grinding location (GL) data of each grinding process.

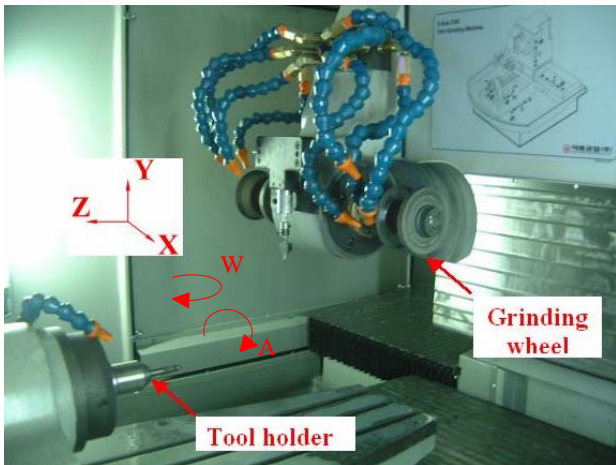


Fig. 1 5-axis CNC machine for manufacturing of ball end mill

### 2. Modeling of ball end mill grinding

The surfaces of a ball end mill are composed of cylindrical part and spherical part. The cutting edge curve is formed by spiral curves which are located on the cylindrical and spherical surfaces respectively. To calculate and simulate helical flute grinding process, a coordinate system attached to the ball end mill is employed, the points of helical groove surface can be expressed by  $\bar{R}_T \ X_T \ Y_T \ Z_T$ , and the points on wheel surface profile can be expressed by  $\bar{R}_W \ X_W \ Y_W \ Z_W$  in coordinate system of grinding wheel. Transformation of coordinate system from  $(X_T, Y_T, Z_T)$  to  $(X_W, Y_W, Z_W)$  can be expressed as:

$$\begin{cases} X_T = f_x(X_W, Y_W, Z_W, m) \\ Y_T = f_y(X_W, Y_W, Z_W, m) \\ Z_T = f_z(X_W, Y_W, Z_W, m) \end{cases} \quad (1)$$

Therefore:

$$F \ X_T \ Y_T \ Z_T = 0 \rightarrow F \ X_W \ Y_W \ Z_W \ m = 0 \quad (2)$$

Equation for family surfaces can be expressed by:

$$F[f_x \ X_W \ Y_W \ Z_W \ m \ f_y \ X_W \ Y_W \ Z_W \ m] \begin{bmatrix} f_z \ X_W \ Y_W \ Z_W \ m \end{bmatrix} = 0 \quad (3)$$

The solution of the direct problem deal with the determination of helical groove surface for a given wheel profile is based on condition of contact between the two surfaces that the relative velocity of the surfaces at the contact points must be orthogonal to the normal vector:

$$\bar{N} \bar{V} = \left( \frac{\partial F}{\partial X_T} \bar{i} + \frac{\partial F}{\partial Y_T} \bar{j} + \frac{\partial F}{\partial Z_T} \bar{k} \right) \left( \frac{\partial f_x}{\partial m} \bar{i} + \frac{\partial f_y}{\partial m} \bar{j} + \frac{\partial f_z}{\partial m} \bar{k} \right) = 0 \quad (4)$$

where  $\bar{V}$  and  $\bar{N}$  are relative velocity of the surface and normal vector of tool surface. Fig.2 shows the simulation result of cross section of helical flute on the cylindrical part.

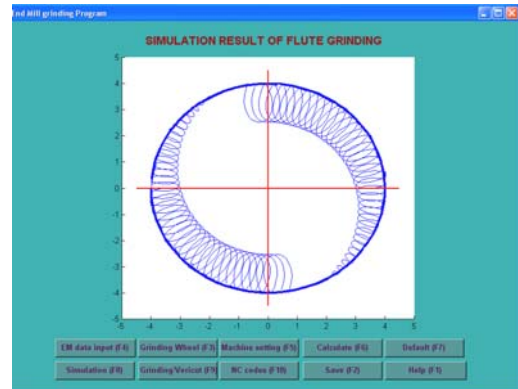


Fig. 2. Cross section of helical flute (back view)

Fig. 3 (a), (b) and (c) show geometry of ball end mill including cutting edge curve, rake face and clearance face. The points M on cutting edge curve can be expressed as a function of helix angle  $\alpha$  and rotation angle  $\phi$  as following equations [4]:

$$M = \begin{pmatrix} -R \sin \alpha \cos \phi & k & 1 - c \sin \phi & \sin \phi \\ -R \cos \alpha \cos \phi & k & 1 - c \sin \phi & \sin \phi \\ -R \sin \alpha \sin \phi & k & 1 - c \cos \phi & \cos \phi \\ -R \cos \alpha \sin \phi & k & 1 - c \cos \phi & \cos \phi \end{pmatrix} \quad 0 \leq \phi \leq \pi \quad (5)$$

where  $k = a \alpha_s$ ,  $R$  and  $\alpha_s$  are radius and helix angle of the cylindrical end mill. Fig. 3 (d) shows calculated results of cutting edge curve with the changing of  $\alpha$  and  $\phi$ . In the ball grinding processes, in order to form a spiral cutting edge, the contact point between the grinding wheel and the cutting edge curve should move along the cutting edge curve.

Fig. 4 shows an illustration for grinding the first clearance face of the ball end mill. The grinding process starts at point S. During the grinding process, the movements of grinding wheel are complex, multi-axis control are required (X, Y, Z, A, W). At final position, the grinding wheel contacts with the machined surface of ball end mill at grinding point E on the wheel surface. Fig. 5 shows relative position between ball end mill and grinding wheel. The relative positions between grinding wheel and ball end mill are controlled by the combination of movements of five axes to perform complex grinding processes. At the contact points between ball end mill and wheel surfaces, three following conditions must be satisfied:

$$\bar{R}_T \ X_T \ Y_T \ Z_T = \bar{R}_W \ X_W \ Y_W \ Z_W \quad (6)$$

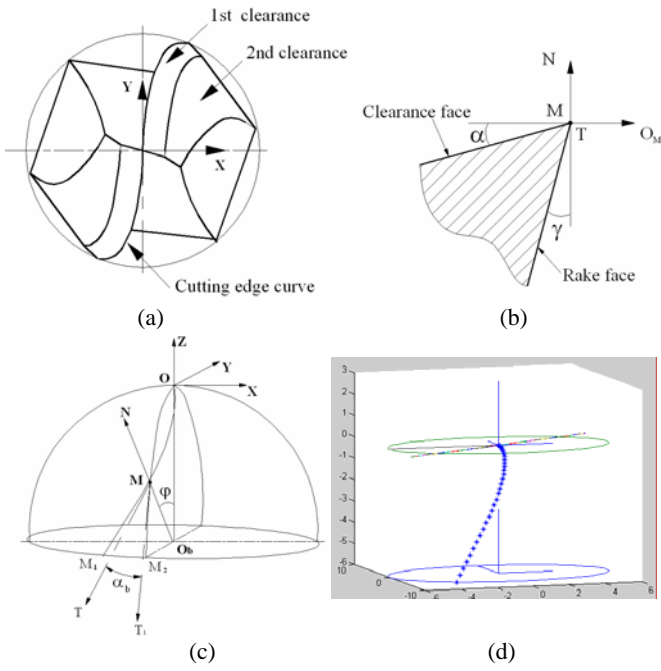


Fig. 3 Geometry of the ball part

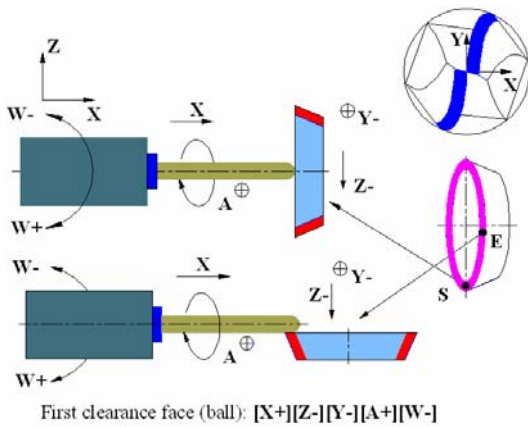


Fig. 4. Scheme for grinding the first clearance face of the ball part

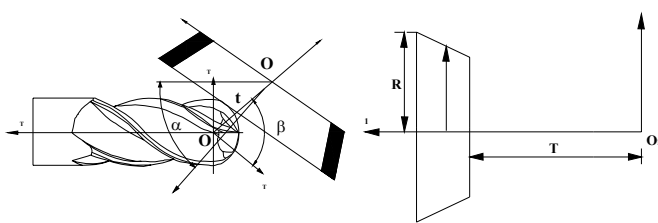


Fig. 5 Relative position between ball end mill and wheel

The relative velocity of the surfaces at the contact points must be orthogonal to the normal vector, when the relative movements are combination of complex motions such as  $\bar{V} = \bar{V}_1 + \bar{V}_2$ , the condition at contact points becomes:

$$\bar{N}\bar{V}_\Sigma = \bar{N}\bar{V}_1 + \bar{N}\bar{V}_2 = 0 \quad (7)$$

To avoid over cutting and non-cutting situations, the relative velocity in normal direction at grinding points must satisfy:

$$\bar{V}_N = \frac{d\bar{N}}{dn} = 0 \quad (8)$$

Fig.6 displays an explanation of relative movement between ball end mill and wheel in ball part grinding processes. The position of point M can be represented as:

$$\bar{R}_{u v} = (X_{u v} \ Y_{u v} \ Z_{u v}) \quad (9)$$

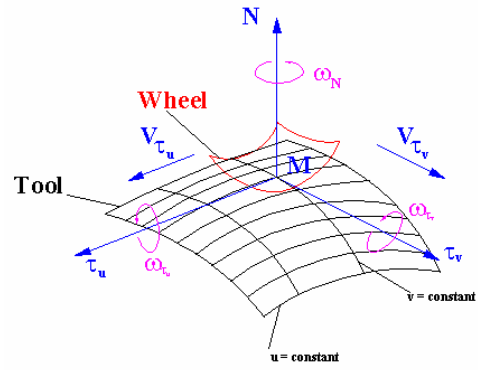


Fig. 6 Movement of wheel in grinding processes.

Considering tangential surface, normal vector at a point in surface,

$$\bar{\tau}_u = \frac{\partial \bar{R}}{\partial u} \times \bar{v}; \quad \bar{\tau}_v = \frac{\partial \bar{R}}{\partial v} \times \bar{u} \quad (10)$$

Normal vector at M can be calculated as:

$$\bar{N} = \frac{\partial \bar{R}}{\partial u} \times \frac{\partial \bar{R}}{\partial v} \quad (11)$$

### 3. imulation of all end mill grinding.

The NC codes which include initial and final position of each axis for all grinding processes of ball end mill are calculated and generated from the software and then will be used to simulate all grinding processes in 3D by using Vericut as shown in Fig. 7

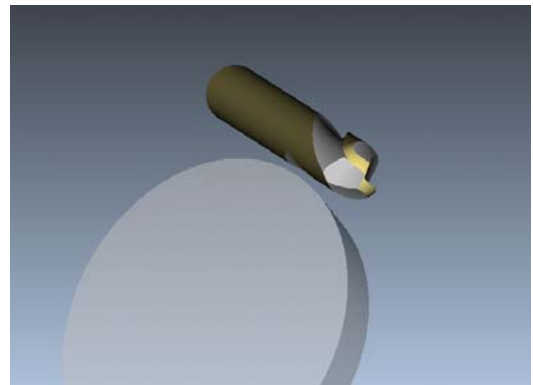


Fig. 7 Simulation result of ball end mill grinding.

### 4. onclusion.

The modeling and simulation for manufacturing of ball end mill presented in this paper provide a practical and efficiency method to develop the computer software for designing, predicting ball end mill geometry before machining, and manufacturing of ball end mill using 5-axis CNC grinding machine.

### References

1. W.F. Chen, H.Y. Lai and C.K. Chen, "A Precision Tool Model for Concave Cone-End Milling Cutters", Int J Adv Manuf Technol 18:567-578, 2001.
2. S.K. Kang, K.F. Ehmman, C. Lin, "A Cad approach to helical groove machining part 1: mathematical model and model solution", International Journal of Machine Tools and Manufacture 36: 141-153, 1996.
3. X. Feng and B. Hongzan, "CNC Rake Grinding for a Taper Ball-End Mill with a Torus-Shaped Grinding Wheel", Int J Adv Manuf Technol 21:549-555, 2003.
4. Yi Lu · Yoshimi Takeuchi · Ichiro Takahashi · Masahiro Anzai, "An integrated system development for ball end mill design, creation and evaluation", Int J Adv Manuf Technol 25: 628-646, 2005